

# Temperature-time profiles of a tubular bus in shorting conditions

**Abstract.** In the paper temperature-time profiles generated in a tubular bus under short-circuit conditions were determined. The initial-boundary parabolic problem was the mathematical model. Adiabatic boundaries of the system and field uniformity at the initial moment of shorting were assumed and motivated. The two models of the bus-bar electric resistivity were considered: the temperature dependent (variable) and averaged one (constant). The problem was solved by means of Green's function. The one-second shorting current and its multi-second equivalents were determined based on the above. The analytical results were verified numerically by the finite element method.

**Streszczenie.** W artykule wyznaczono czasowe przebiegi temperatury generowane w szynoprzewodzie rurowym podczas zwarcia. Matematycznym modelem jest początkowo-brzegowe zagadnienie paraboliczne. Przyjęto i uzasadniono założenie o adyabatycznych brzegach układu oraz o równomierności pola w początkowej chwili zwarcia. Rozpatrywano dwa modele elektrycznej rezystywności szynoprzewodu: uzależnionej termicznie (zmiennej) i uśrednionej (stałej). Zagadnienie rozwiązano za pomocą funkcji Greena. Na tej podstawie wyznaczono jednosekundowy prąd zwarcia i jego wielosekundowe równoważniki. Wyniki analityczne zweryfikowano numerycznie metodą elementu skończonego. (Przebiegi temperatury szynoprzewodu rurowego w warunkach zwarciovych).

**Keywords:** tubular bus, shorting, temperature-time profile, Green's function, one-second shorting current

**Słowa kluczowe:** szynoprzewód rurowy, zwarcie, przebiegi temperatury, funkcja Greena, jednosekundowy prąd zwarcia

## Introduction

The heated tubular bus in rated conditions was analysed in paper [1]. The mentioned conditions cause that the heating curves are similar to the diagrams of increasing exponential functions. Besides, thermal field values did not exceed a maximum operating temperature. At the present article the thermal field is investigated under short-circuit conditions. Obtained temperature-time profiles are totally different from those determined in [1]. Namely, they are similar to diagrams of the linear functions, they grow much faster and to bigger values than those in [1]. Besides, the time of shorting is incomparably shorter from the time of the system heating-up in nominal rating conditions. Then, the aim of the presented paper is an investigation of the thermal field picture in the case of substitution of the rating conditions [1] by the shorting ones. The additional aim is determination of the one-second shorting current (and its multi-second equivalents). That parameter has important significance because of the risk of the thermal destruction of the power connections and contacts.

The analysed bus-bar is presented in Fig. 1, [15, Fig.1]. The system is a seamless, hollow cylinder of internal radius  $R_1$  and external  $R_2$ . The length of a tube is much larger than its exterior diameter  $2R_2$  (60:1). It follows from the above the axiallysymmetrical configuration of a bus-bar. The thermal field is generated by the flow of a shorting current of the rms value  $I_{sh}$  and of the power frequency  $f=60Hz$ .

Temperature influence on the thermal conductivity  $\lambda_{sh}$  and on the specific heat  $c_{sh}$  of metals (Cu or Al) is relatively small [2], [3]. For this reason the parameters  $\lambda_{sh}$  and  $c_{sh}$  may be averaged within the assumed range of temperature variations (from  $70^\circ C$  to  $110^\circ C$ ). However the above remark does not consider the resistivity  $\rho(T_{sh})$  of a bus-bar. With a sufficient accuracy  $\rho(T_{sh})$  may be approximated by the following function

$$(1) \quad \rho(T_{sh}) = \rho(T_1) [1 + \varepsilon * (T_{sh} - T_1)] \quad \text{for } T_{sh} < 200^\circ C,$$

where  $\rho(T_1) = \rho(20^\circ C) [1 + \varepsilon (T_1 - 20^\circ C)]$  denotes the resistivity at temperature  $T_1$  [4],  $T_{sh}$  is the temperature during a shorting and  $\varepsilon^* = \varepsilon / [1 + \varepsilon (T_1 - 20^\circ C)]$ . In case of copper  $\rho(20^\circ C) = 1.71 \cdot 10^{-8} \Omega m$  and  $\varepsilon = 39.3 \cdot 10^{-4} 1/^\circ C$ .

The last parameter means the temperature resistivity coefficient.

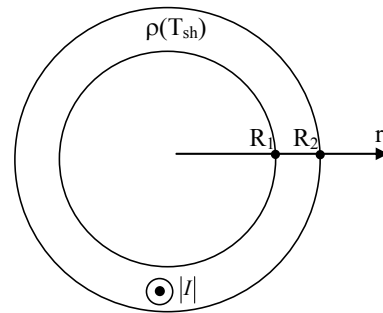


Fig. 1. Cross-section of a tubular bus

## Boundary-initial problem of the thermal field generated by shorting current

The volume power density of a source is  $g=P/V$ , where  $P = R_{AC} |I_{sh}|^2 = k_s R_{DC} |I_{sh}|^2 = k_s \rho(T_{sh}) |I_{sh}|^2 / [\pi(R_2^2 - R_1^2)]$  means the active power,  $R_{AC}$ ,  $R_{DC}$  are electric resistances of the bar for the AC and DC current respectively,  $k_s$  denotes a coefficient of the skin-effect [4],  $l$  represents a length of the system and  $V = \pi(R_2^2 - R_1^2)l$  is the volume of a hollow cylinder. Considering the above in the balance of an energy together with (1) and assumptions from the previous chapter the following parabolic equation was obtained [3] with respect to a temperature increase  $v_{sh}(r,t) = T_{sh}(r,t) - T_a$ ,  $T_1 = T_a$

$$(2) \quad \frac{\partial^2 v_{sh}(r,t)}{\partial r^2} + \frac{1}{r} \frac{\partial v_{sh}(r,t)}{\partial r} - \frac{1}{\chi_{sh}} \frac{\partial v_{sh}(r,t)}{\partial t} + m v_{sh}(r,t) = -\frac{g_a}{\lambda_{sh}}$$

for  $R_1 \leq r \leq R_2$ ,  $t \geq 0$ , where  $r$  is the radial coordinate,  $t$  is a time,  $\chi_{sh}$  denotes the diffusivity  $\lambda_{sh}/(c_{sh}\mu_{sh})$ ,  $\mu_{sh}$  represents the mass density,

$$m = \frac{\rho(T_a) \varepsilon^* |I_{sh}|^2 k_s}{\pi^2 (R_2^2 - R_1^2)^2 \lambda_{sh}}, \quad \rho(T_a) = \rho(T_1 = T_a),$$

$\varepsilon^* = \varepsilon * (T_1 = T_a)$ ,  $T_a$  is an ambient temperature and

$g_a = \frac{\rho(T_a) |I_{sh}|^2 k_s}{\pi^2 (R_2^2 - R_1^2)^2}$  denotes the volume density of power of a heat source at temperature  $T_a$ .

The additional component should be noticed in equation (2) (i.e. the last term on the left side). It results from consideration of relation (1) and it is not appeared in a classic equation of the heat conduction [5], [6]. This way a solution of the problem is more complicated.

Due to thermal inertia the system will not manage to give up heat during a short circuit [7], [8]. In the mathematical sense, this is expressed by the relation between short circuit duration  $t_{sh}$  (max. 5s) and thermal time constant  $\tau_H(r)$  (3027.4s, [1, section 3.3]). Therefore, inequality  $t_{sh} \ll \tau_H(r)$  is satisfied. Consequently, the boundary conditions on  $r=R_1$  and  $r=R_2$  surfaces can be assumed adiabatically for  $t \leq t_{sh}$

$$(3) \quad \left. \frac{\partial v_{sh}(r,t)}{\partial r} \right|_{r=R_1} = \left. \frac{\partial v_{sh}(r,t)}{\partial r} \right|_{r=R_2} = 0$$

for  $R_1 \leq r \leq R_2, t \leq t_{sh}$ .

It was assumed that a short circuit takes place in the steady state generated by rated current. The material of the tubular bus is characterised by great thermal and electric conductivity (Cu or Al) and the majority of the thermal resistance resides in the convective layer outside of the conductor. Therefore, in the initial moment of a short circuit one can assume a uniform temperature distribution in the system's cross-section

$$(4) \quad v_{sh}(r, t=0) = T_{max} - T_a \quad \text{for } R_1 \leq r \leq R_2,$$

where  $T_{max}$  means sustained maximum temperature (or maximum operating temperature).

New function  $w_{sh}(r,t)$  [9] was introduced to eliminate the fourth term of the left hand side (2)

$$(5) \quad v_{sh}(r,t) = w_{sh}(r,t) \cdot e^{m\chi_{sh}t}.$$

After substituting (5) to equation (2) the following was obtained

$$(6) \quad \frac{\partial^2 w_{sh}(r,t)}{\partial r^2} + \frac{1}{r} \frac{\partial w_{sh}(r,t)}{\partial r} - \frac{1}{\chi_{sh}} \frac{\partial w_{sh}(r,t)}{\partial t} = -\frac{g_a}{\lambda_{sh}} e^{-m\chi_{sh}t}$$

for  $R_1 \leq r \leq R_2, t \geq 0$ .

On the other hand, after considering (5) the form of boundary condition (3) and initial condition (4) does not change. In order to obtain them it is enough to make change  $v_{sh}(r,t) \rightarrow w_{sh}(r,t)$  in relations (3), (4).

### Green's function of the heating model in short-circuit conditions

The boundary-initial problem for Green's function  $G_{sh}=G_{sh}(r,t,\xi,\eta)$  [9], [10], [11] was defined as down below

$$(7) \quad \frac{\partial^2 G_{sh}}{\partial r^2} + \frac{1}{r} \frac{\partial G_{sh}}{\partial r} - \frac{1}{\chi_{sh}} \frac{\partial G_{sh}}{\partial t} = -\frac{1}{r\chi_{sh}} \delta(r-\xi) \delta(t-\eta)$$

for  $R_1 \leq r \leq R_2, t \geq \eta$ ,

$$(8) \quad \left. \frac{\partial G_{sh}}{\partial r} \right|_{r=R_1} = \left. \frac{\partial G_{sh}}{\partial r} \right|_{r=R_2} = 0 \quad \text{for } t \geq \eta,$$

$$(9) \quad G_{sh} = 0 \quad \text{for } t \leq \eta,$$

where the product of shifted Dirac's impulses is on the right side of (7).

After taking into considerations boundary conditions (8), the initial one (9) and analogical ones for function  $w_{sh}(r,t)$  (obtained after exchange  $v_{sh}(r,t) \rightarrow w_{sh}(r,t)$  in (3), (4)) it is obtained [9], [11]

$$(10) \quad w_{sh}(r,t) = \int_{R_1}^{R_2} G_{sh}(r,t,\xi,\eta=0) (T_{max} - T_a) \xi d\xi + \frac{\chi_{sh}}{\lambda_{sh}} \int_0^t \int_{R_1}^{R_2} g_a e^{-m\chi_{sh}\eta} G_{sh}(r,t,\xi,\eta) \xi d\xi d\eta.$$

In comparison with [1, (14)], the additional summand occurs in (10) which is connected with non-zero initial condition (4).

In order to determine Green's function, the homogeneous auxiliary problem was introduced [9] towards function  $\Psi_{sh}(r,t)$

$$(11) \quad \frac{\partial^2 \Psi_{sh}(r,t)}{\partial r^2} + \frac{1}{r} \frac{\partial \Psi_{sh}(r,t)}{\partial r} - \frac{1}{\chi_{sh}} \frac{\partial \Psi_{sh}(r,t)}{\partial t} = 0$$

for  $R_1 \leq r \leq R_2, t \geq 0$ ,

$$(12) \quad \left. \frac{\partial \Psi_{sh}(r,t)}{\partial r} \right|_{r=R_1} = \left. \frac{\partial \Psi_{sh}(r,t)}{\partial r} \right|_{r=R_2} = 0 \quad \text{for } t \geq 0,$$

$$(13) \quad \Psi_{sh}(r,0) = F(r) \quad \text{for } R_1 \leq r \leq R_2,$$

where  $F(r)$  is any distribution of the initial condition.

The auxiliary problem (11)-(13) was solved with two methods: separation of variables [5], [12] and Green's function [9], [10]. In the solution obtained by the separation of variables method there is a additional eigenvalue [6]. This results from the boundary condition of the second kind (12). Then a constant element exist in the front of series in the solution (as a counterpart of the additional eigenvalue). After comparing the solutions and replacing  $t \rightarrow t-\eta$  there was Green's function of the heating model in short-circuit conditions obtained

$$(14) \quad G_{sh}(r,t,\xi,\eta) = \frac{2}{R_2^2 - R_1^2} + \sum_{n=1}^{\infty} \frac{2\Lambda_0 \left( \kappa_n \frac{\xi}{R_1} \right) \Lambda_0 \left( \kappa_n \frac{r}{R_1} \right) \cdot e^{-\frac{\kappa_n^2}{R_1^2} \chi_{sh} (t-\eta)}}{R_2^2 \Lambda_0^2 \left( \kappa_n \frac{R_2}{R_1} \right) - R_1^2 \Lambda_0^2 (\kappa_n)}$$

for  $R_1 \leq r \leq R_2, t \geq \eta$

where

$$(15) \quad \Lambda_p \left( \kappa_n \frac{r}{R_1} \right) = J_p \left( \kappa_n \frac{r}{R_1} \right) Y_1 \left( \kappa_n \frac{R_2}{R_1} \right) - Y_p \left( \kappa_n \frac{r}{R_1} \right) J_1 \left( \kappa_n \frac{R_2}{R_1} \right),$$

while  $\kappa_n$  is determined by means of the following equation of eigenvalues

$$(16) \quad \Lambda_1(\kappa_n) = 0 \quad \text{for } \kappa_n > 0.$$

### Shorting temperature-time profiles and short duration fault currents

Green's function (14) was substituted into (10) and integrated. In order to achieve that, one used equation of eigenvalues (16) and definition (15). As the result, both

series reduced to zero except for the constant component (corresponding with additionally eigenvalue). Subsequently, the obtained result was substituted into (5) and the increase definition given before formula (2) was applied. Eventually, the heating curves in short-circuit condition were obtained

$$(17) \quad T_{sh}(t) = T_a + (T_{\max} - T_a)e^{m\lambda_{sh}t} + \frac{g_a}{m\lambda_{sh}}(e^{m\lambda_{sh}t} - 1) \quad \text{for } t \leq t_{sh}.$$

Temperature-time history (17) and other parameters of the system were calculated in Mathematica 10.4 software [13]. The following data were assumed

$$(18) \quad R_1 = 0.04445m, \quad R_2 = 0.0508m, \quad \lambda_{sh}(90^\circ C) = 379.3 \text{ W/(mK)}, \\ c_{sh}(90^\circ C) = 402.3 \text{ J/(kgK)}, \quad \mu_{sh} = 8940 \text{ kg/m}^3, \quad k_s = 1.02, \quad T_a = 40^\circ C, \\ \rho(40^\circ C) = 1.8444 \cdot 10^{-8} \Omega m, \quad \varepsilon^* = 36.4361 \cdot 10^{-4} \text{ } 1^\circ C., \quad T_{\max} = 70^\circ C,$$

The essentials parameters are: one-second shorting current and its multi-second equivalents. These are determined from the following condition: in the moment of shorting interruption ( $t = t_{sh}$ ) the temperature of the bus does not exceed limiting value  $T_{SH}$ . The discussed example assumed  $T_{SH} = 110^\circ C$ . Such values assures thermal safety of power connections and contacts [16]. As temperature is an increasing function of short-circuit current, one should only solve the following equation towards  $|I_{sh}|$

$$(19) \quad T_{SH} = T_{sh}(t = t_{sh}, |I_{sh}| = I_{sh}).$$

Respective shorting currents were calculated on the basis of (17), (19). The iterative method and While loops in Mathematica software [13] were used. Shorting current  $I_{sh1} = 152 \text{ } 921A$  was obtained for the one-second short circuit,  $I_{sh3} = 88 \text{ } 289A$  for the three-second short circuit and  $I_{sh5} = 68 \text{ } 388A$  for the five-second one. Fig. 2 shows temperature changes illustrated with a heavy line for the aforementioned currents at different shorting duration. In power installations, the determined ampacity should be reduced due to the electrodynamic forces and thermal strength of other components of the current carrying path (such as transformers, conductors, line traps and switches). With regard to a lack of radial coordinate in (17), temperature changes are the same throughout the whole cross-section of the system.

For comparison purposes, the same characteristics and parameters were determined again but at constant (averaged) resistivity in the scope of temperature changes from  $70^\circ C$  to  $110^\circ C$  (that is,  $\rho(T_{av} = 90^\circ C) = 2.1804 \cdot 10^{-8} \Omega m$ ). In this case, a equivalent temperature coefficient of resistivity should be set to zero ( $\varepsilon = 0 \Rightarrow \varepsilon^* = 0$ ). Then, the following results from relations given below formula (2)

$$(20) \quad m = 0 \quad \text{and} \quad g_a \rightarrow g_{av} = \frac{\rho(T_{av})|I_{sh}|^2 k_s}{\pi^2(R_2^2 - R_1^2)}.$$

After considering (20) with proper indexing and calculating the limit of function (17) the following was obtained

$$(21) \quad T(t) = \lim_{\substack{m \rightarrow 0 \\ g_a \rightarrow g_{av}}} T_{sh}(t) = T_{\max} + \frac{g_{av}\lambda_{sh}}{\lambda_{sh}} t \quad \text{for } t \leq t_{sh},$$

where  $T(t)$  means linear dependence of the temperature of the tubular bus during a short circuit at averaged resistivity  $\rho(T_{av} = 90^\circ C)$ . Graph of function (21) is presented in Fig. 2. by means of dashed lines (at the same currents as for variable (temperature dependent) resistivity  $\rho(T_{sh})$ ).

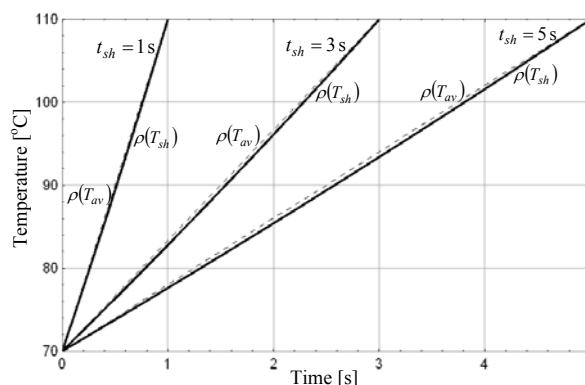


Fig. 2. Time profiles of temperature in the tubular bus at variable  $\rho(T_{sh})$  and averaged  $\rho(T_{av} = 90^\circ C)$  resistivity for the one-second shorting and current load  $I_{sh1} = 152 \text{ } 921A$ , for the three-second short circuit at  $I_{sh3} = 88 \text{ } 289A$  and the five-second one at  $I_{sh5} = 68 \text{ } 388A$

### Numerical verification of the solution

The presented method was verified. For the verification purposes, the obtained results were compared with numerical calculations done with Mathematica 10.4 software [13]. Namely, with the use of the finite element method [14], problem (2)-(4) converted into temperature was solved again. Subsequently, the relative differences of temperature increases were calculated according to the following formula

$$(22) \quad \delta_T = 100\% \frac{[T_{sh}(t) - T_a] - [T_{FE}(t) - T_a]}{[T_{sh}(t) - T_a]},$$

where  $T_{sh}(t)$  represents temperature-time profile obtained with Green's method,  $T_{FE}(t)$  is temperature-time history calculated with finite element method,  $T_a$  denotes reference temperature (ambient temperature in this case). Fig. 3 shows relation (22) at variable (temperature depended) resistivity of the tubular bus for different short circuit duration.

### Final remarks

Short but intense heating with fault current make time profiles of temperature throughout the whole cross-section of the tubular bus almost linear (Fig. 2). Averaging resistivity  $\rho(T_{av})$  results in an inconsiderable increase in temperature compared to case  $\rho(T_{sh})$  in the short-circuit analysis (in Fig. 2, dashed lines are placed higher than heavy ones). It can be noticed, that for the shorter duration of a shorting the speed raising of the curves  $\rho(T_{av})$  and  $\rho(T_{sh})$  is considerably growing when current becomes larger (Fig. 2 for  $t_{sh} = 1s, 3s, 5s$ ).

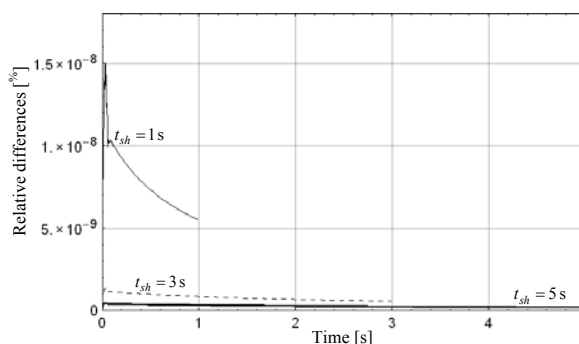


Fig. 3. Relative differences of temperature increases determined by the finite element and Green's methods for different short circuit duration at variable (temperature depended) resistivity  $\rho(T_{sh})$

Relative differences (22) (of temperature increases calculated by means of the finite element and Green's methods) are very small (Fig. 3). Some more discrepancy seen for the one-second shorting (Fig. 3,  $t_{sh}=1s$ ) results from a very large speed of temperature rising in that case. Despite of that Fig. 3 illustrates an excellent conformity of the analytic and numerical solution.

#### ACKNOWLEDGEMENT

The paper was prepared at Białystok Technical University within a framework of the S/WE/2/2018 project sponsored by the Ministry of Science and Higher Education, Poland.

**Authors:** prof. J. Gołębiowski<sup>1</sup>, D.Sc., Ph.D., M. Zaręba<sup>2</sup>, Ph.D., Białystok University of Technology, Faculty of Electrical Engineering, Department of Theoretical Electrotechnics and Measurements, 15-351 Białystok, 45 D Wiejska Street, Poland, e-mail: <sup>1</sup>j.golebiowski@pb.edu.pl, <sup>2</sup>m.zareba@pb.edu.pl

#### REFERENCES

- [1] Gołębiowski J., Zaręba M., Analytical modelling of the transient thermal field of a tubular bus in nominal rating, *COMPEL: The International Journal for Computation and Mathematics in Electrical and Electronic Engineering*, 38 (2019), no.2, 642-656, <https://doi.org/10.1108/COMPEL-02-2018-0078>.
- [2] Ashcroft N.W., Merlin N.D., Solid state physics, *Holt-Saunders International Editions*, Japan (1981).
- [3] Hoffer O., Instationäre Temperaturverteilung in Einem Runddraht, *Archiv für Elektrotechnik*, 60 (1978), no.6, 319-325.
- [4] Anders G.J., Rating of electric power cables: ampacity computations for transmission, distribution, and industrial applications, *McGraw-Hill Professional*, New York (1997).
- [5] Kącki E., Równania różniczkowe cząstkowe w zagadnieniach fizyki i techniki (Partial differential equations in the problems of physics and technology), *WNT*, Warszawa (1992).
- [6] Hahn D.W., Ozisik M.N., Heat Conduction, *John Wiley and Sons*, New Jersey (2012).
- [7] Markiewicz H., *Urządzenia elektroenergetyczne* (Electric power devices), *WNT*, Warszawa (2016).
- [8] Kulas S., Tory prądowe i układy zestykowe (Current ducts and contact systems), *Oficyna Wydawnicza Politechniki Warszawskiej*, Warszawa (2008).
- [9] Cole K.D., Haji-Sheikh A., Beck J.V., Litkouhi B., Heat conduction using Green's functions, *CRC Press-Taylor and Francis Group*, Boca Raton-London-New York (2011).
- [10] Duffy D.G., Green's functions with applications, *CRC Press* (2015).
- [11] Greenberg M.D., Applications of Green's function in science and engineering, *Dover Publications*, USA (2015).
- [12] Latif M.J., Heat conduction, *Springer-Verlag*, Berlin, Haidelberg (2009).
- [13] Wolfram Research Inc., Mathematica, version 10.4, *Champaign, Illinois* (2016).
- [14] Nithiarasu P., Lewis R.W., Seeharamu K.N., Fundamentals of the finite element method for heat and mass transfer, *John Wiley and Sons Ltd.*, New Jersey (2016).
- [15] Coneybeer R.T., Black W.Z., Bush R.A., Steady-state and transient ampacity of bus bar, *IEEE Transactions on Power Delivery*, 9(1994), no.4, 1822-1829.
- [16] Nawrowski R., *Tory wielkoprądowe izolowane powietrzem lub SF<sub>6</sub>* (Air-insulated or SF<sub>6</sub> high current busbars), *Oficyna Wydawnicza Politechniki Poznańskiej*, Poznań (1998).